molecules, like ethylene, have been converted into paraffins and aromatics over faujasite-type zeolites (Venuto et al., 1966).

Reactions c and d involve carbonium ions and require the presence of acid sites. There is spectroscopic evidence for the interaction of zeolitic acidic OH groups with π-electron systems of adsorbed olefins and aromatics (Venuto and Landis, 1968). Such an interaction is likely to facilitate the subsequent conversion of these molecules, leading to paraffins and condensed, hydrogen-deficient aromatics (coke). This explains why over strongly acidic zeolites, such as RE,H-Y, the rate of these hydrogen-transfer reactions is high. The presence of metals also facilitates these reactions.

We have shown that USY zeolites have a lower overall acidity than RE,H-Y zeolites. The lower density of acid sites in USY zeolites reduces the rate of conversion of olefins into paraffins and of aromatics into condensed polycycles, thus allowing the olefins and aromatics to diffuse out of the zeolite and to desorb. The higher content in aromatic and allylic hydrocarbons in the gasoline fraction obtained from gas oil cracking over ultrastable zeolites, as well as the lower coke yield and higher olefin selectivity, is in agreement with this interpretation.

Exchange of rare earth into the zeolite will increase the rate of these hydrogen-transfer reactions, resulting in more coke and higher conversions. This effect will be more pronounced as the rare earth content of the ultrastable zeolite increases.

The data presented show that the rare earth-exchanged USY zeolites combine the catalytic properties of USY zeolites with those of RE,H-Y. By varying the rare earth input into the zeolite, a series of yield-oriented catalysts can be prepared, each tailored to meet the demand of a particular segment of the refining industry.

Acknowledgment

The authors express their appreciation to the Davison Division of W. R. Grace & Co. for permission to publish the results of this study.

Literature Cited

Ciapetta, F. G., Henderson, D., *Oil Gas J.*, 88 (Oct 16, 1967).
Hirschler, A. E., *J. Catal.*, **2**, 428 (1963).
John, T. M., Wojciechowski, B. W., *J. Catal.*, **37**, 240, 348, 358 (1975).
Magee, J. S., Blazek, J. J., Ritter, R. E., *Oil Gas J.*, 48 (July 23, 1973).
Magee, J. S., Blazek, J. J., *ACS Monogr.*, **No. 171**, 646 (1976).
Moscou, L., Moné, R., *J. Catal.*, **30**, 471 (1973).
Nace, D. M., *Ind. Eng. Chem. Prod. Res. Dev.*, **8**, 37 (1969).
Name, D. M., *Ind. Eng. Chem. Prod. Res. Dev.*, **9**, 203 (1970).
Pickert, P. E., Rabo, J. A., Dempsey, E., Schomaker, V., *Proc. Int. Congr. Catal., 3rd, 1964*, **1**, 714 (1965).
Plank, C. J., *Proc. Int. Congr. Catal., 3rd, 1964*, **1**, 727 (1965).
Plank, C. J., Rosinski, E. J., Hawthorne, W. P., *Ind. Eng. Chem. Prod. Res. Dev.*, **3**, 165 (1964).
Richardson, J. T., *J. Catal.*, **9**, 182 (1967).
Scherzer, J., Bass, J. L., *J. Catal.*, **46**, 100 (1977).
Thomas, C. L., Barmby, D. S., *J. Catal.*, **12**, 341 (1968).
Tung, S. E., McIninch, E., *J. Catal.*, **10**, 166, 175 (1968).
Venuto, P. B., Hamilton, L. A., Landis, P. S., *J. Catal.*, **5**, 484 (1966).
Venuto, P. B., Landis, P. S., *Adv. Catal.*, **18**, 303 (1968).
Wang, I., Ph.D. Thesis, University of Utah, 1974.

Received for review December 7, 1977
Accepted May 30, 1978

Synthesis of Mordenite Type Zeolite

Pramod K. Bajpai and M. Someswara Rao*

Department of Chemical Engineering, Indian Institute of Technology, Kanpur-208016, U.P., India

K. V. G. K. Gokhale

Department of Civil Engineering, Indian Institute of Technology, Kanpur-208016, U.P., India

In spite of the availability of vast literature on mordenite type zeolite, information on its synthesis and stability, and also the role of different parameters on its formation, is limited. In the present investigation the mordenite was synthesized between 135 and 165 °C involving several compositions for starting mixture, temperature, and varied periods of time. The roles of different parameters such as the composition of the starting mixture, temperature, and duration of synthesis on the formation of sodium mordenite and its stability are investigated. The progress of the reaction for different conditions was tracked using X-ray diffraction technique, and the crystallization kinetics for mordenite formation was also studied.

Introduction

The utilization of synthetic crystalline zeolites as molecular sieves and as catalysts finds extensive potential in adsorption separations, ion exchange, hydrocarbon catalysis, recovery of radioactive ions from waste solutions, separation of hydrogen isotopes, and other purifications (Breck, 1974; Kladning, 1975). The internal pore space available in any particular zeolite is governed by its structure. The zeolites are characterized by the general formula $M_{x/n}[(AlO_2)_x \cdot (SiO_2)_y] \cdot wH_2O$, where M is the exchange cation of valency n, w is the number of water molecules, and $x + y$ is the total number of tetrahedra per unit cell. The ratio y/x ranges between 1 and 10 for natural and synthetic zeolites. These are structurally classified according to the openness of their framework as measured by their water sorption capacity (Meier, 1968; Barrer, 1968). Mordenite type zeolites have a water sorption capacity of 0.27–0.33 cm^3 of H_2O/cm^3 of zeolite. Several forms of mordenite reported in literature are the derivatives of the original sodium form after ion exchange. The unit cell of the sodium form of mordenite has the dimensions: a = 18.13 Å, b = 20.49 Å, and C = 7.52 Å, and

0019-7890/78/1217-0223$01.00/0

its chemical constitution (Meier, 1961) is represented by

$$(Na_2O)_4 \cdot (Al_2O_3)_4 \cdot (SiO_2)_{40} \cdot 24H_2O$$

Although mordenite occurs in nature as a mineral, synthetic mordenites, owing to their purity, are better suited to meet the stringent requirements imposed on molecular sieve adsorbents in adsorption and catalytic processes. Of the available commercial molecular sieve adsorbents currently in use, the mordenite molecular sieves, being high in their silica/alumina ratio, are preferred for use where acidic components are involved. As catalysts, mordenite type zeolites find applications in a variety of reactions. For example, the hydrogen mordenite is used for isomerization of xylenes and cyclohexane (Hansford and Ward, 1969; Hopper and Shigemura, 1973; Voorhies and Hopper, 1971; Allan and Voorhies, 1972). The mordenite catalysts are also used for alkylation, disproportionation, trans-alkylation, dehydration, steam reforming, polymerization, and a host of other reactions (Keough and Sand, 1961; Brecker et al., 1973; Karge, 1973; Tatsuaki et al., 1970; Brooks, 1971; Kawasaki et al., 1971; Miale and Weisz, 1971).

Considerable published literature as well as patents are available on the synthesis of mordenite type zeolite (Barrer, 1948; Barrer and White, 1952; Ames and Sand, 1958; Domine and Quobex, 1968; Sand et al., 1971; Wolf and Renning, 1971; Norton Co., 1965). Several starting materials of both chemical and natural sources have been used in the synthesis. Barrer (1948, 1951, 1952) has carried out extensive pioneering work on the hydrothermal chemistry of aluminosilicates. In spite of the availability of vast published literature, information on the synthesis and stability of mordenite as also the role of the different parameters in its formation is extremely limited. In the present investigation, the role of different parameters such as composition of the starting mixture, temperature, and duration of synthesis on the formation of sodium mordenite and its stability are investigated.

Experimental Section

Materials. For the synthesis of zeolites, silica has been used in the form of sodium silicate and silica gel. The sodium silicate contained 29.2 wt % Na_2O and 28.3 wt % SiO_2 as supplied by M/S Chemilon, Bombay, India. Silica gel was used in conjunction with sodium silicate to obtain the required silica content in the initial mixture. The silica gel (obtained from M/S Sarabhai-Merck Chemicals of Baroda, India) was finely ground in a ball mill to the particle size fraction passing through 200 mesh. High purity aluminum hydroxide and sodium hydroxide were supplied by M/s E. Merck AG Darmstadt, West Germany, and Sarabhai-Merck Chemicals of Baroda, India, respectively. Zeolon from the Norton Company (USA) was chosen as a standard for comparing the synthesized mordenite.

Methods. On the basis of preliminary investigations, it has been found that the starting materials in the form of an aluminosilicate gel rather than in the form of individual oxides facilitate better synthesis of mordenite. The sodium aluminosilicate was prepared by mixing sodium aluminate with sodium silicate. Sodium aluminate itself was prepared from the reaction of sodium hydroxide and aluminum hydroxide. If more silica was required, the appropriate quantity of silica gel was added to the sodium silicate before making the gel.

The hot solution of the starting mixture was kept in the autoclave for the hydrothermal reaction. The autoclave used in the present investigation was a high-pressure type of Parr make (series 4500). The autoclave temperature was controlled to an accuracy of ±2 °C. The desired reaction

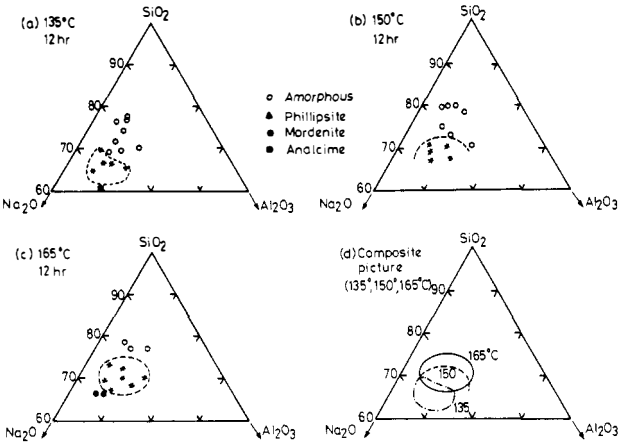

Figure 1. Reaction composition diagrams for 12 h.

temperature was attained within 30–50 min. The zero time of the reaction was corrected adopting the method suggested by Freund (1976). At the end of each run conducted for a specific period of time, the product was filtered and subsequently washed with hot distilled water until the pH of the filtrate reached 7. The solid product was then dried at 120 °C in an oven for 12 h and characterized. In addition to mordenite, the reaction products often included either analcime or phillipsite. The products were identified from their X-ray diffraction patterns on the basis of their characteristic intense reflections. Quantitative estimation of mordenite present in various samples was carried out by the calibration of peak intensities with the standard mordenite.

X-ray diffraction analyses of the synthesized samples were carried out on a G.E. unit fitted with an XRD-6 diffractometer using Ni-filtered Cu Kα radiation. Scanning was done in the range of 6–60° (2θ) at a rate of 2°/min with a chart speed of 1 in./min. The exact peak positions were checked by obtaining the counts from point to point within the peak range. The interplanar spacings (d) were obtained for the synthesized samples and the cell constants were also determined for the mordenite using the formula for the orthorhombic system (McLachlan, 1957).

The IR spectra for the samples as recorded by a Perkin-Elmer 521 IR spectrophotometer using KBr pellet technique (Rao, 1963) were obtained in the frequency ranges for the framework as also the association of water (4000–300 cm^{-1}).

Results and Discussion

In order to study the stability and role of different parameters on the mordenite formation, the following ranges of operating variables were used: temperature of reaction, 90–200 °C; synthesis time, 1 h–4 days; molar ratios in the starting mixture: SiO_2/Al_2O_3, 1–16; Na_2O/Al_2O_3, 0.8–6.0; and H_2O/Al_2O_3, 219.

Effect of Starting Composition. Initial composition of any mixture is of paramount importance in governing the type of zeolite crystallized. In the present investigation, the composition of the starting mixture was varied in the following ranges of the components: Na_2O (mol %), 12.0–50.0; Al_2O_3 (mol %), 4.0–18.0; SiO_2 (mol %), 32.8–80.0; H_2O/Na_2O (molar ratio), 40.0–200.0. To represent the stability fields of mordenite as a function of composition in the system Na_2O–Al_2O_3–SiO_2–H_2O at constant H_2O/Al_2O_3 ratio, triangular diagrams for the temperatures 135, 150, and 165 °C were plotted. These diagrams are given for 12 and 24 h of synthesis periods for these temperatures (Figures 1 and 2).

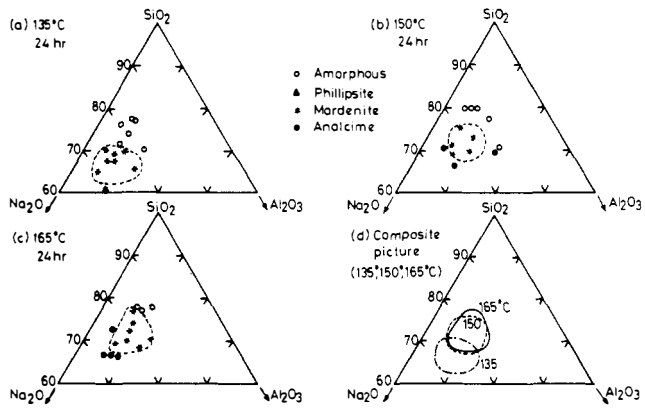

Figure 2. Reaction composition diagrams for 24 h.

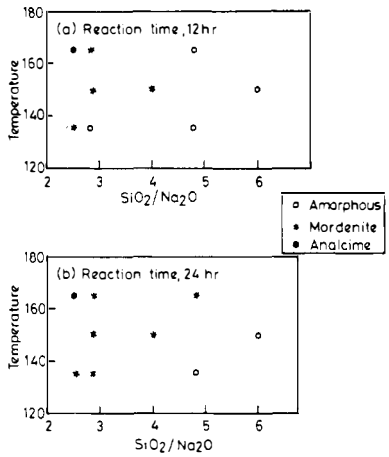

Figure 3. Effect of composition at different temperatures (constant Al_2O_3, 6.7%).

If the SiO_2/Al_2O_3 and Na_2O/Al_2O_3 ratios are plotted against each other for the reaction temperatures of 135, 150, and 165 °C, it will be seen that, temperature and time remaining constant, a higher SiO_2/Al_2O_3 ratio in the starting mixture requires a higher ratio of Na_2O/Al_2O_3 for the formation of mordenite. In any starting mixture with a fixed SiO_2/Al_2O_3 ratio, temperature and time remaining constant, it will also be seen that an increase in the Na_2O/Al_2O_3 ratio results in a shift from mordenite to analcime crystallization. Similarly, an increase in SiO_2/Al_2O_3 ratio for a fixed Na_2O/Al_2O_3 ratio favors the crystallization of mordenite instead of analcime. Similar observations were reported by Barrer (1948, 1952).

From the triangular diagrams (Figures 1 and 2), the effect of composition can also be examined by choosing the tie lines for any particular Al_2O_3 percent and obtaining SiO_2 and Na_2O contents in the starting mixture for different temperatures. The SiO_2/Na_2O ratios are plotted against temperature with the corresponding product phase indicated (Figure 3). From such plots, it is clear that a higher ratio of SiO_2/Na_2O is required for the formation of mordenite at higher temperatures and that at any particular temperature, a decrease in the SiO_2/Na_2O ratio shifts the sequence of product formation in the direction of amorphous to phillipsite/mordenite to analcime. The appearance of mordenite or phillipsite is guided by the availability of silica during the zeolite crystallization. Mordenite in its composition has a SiO_2/Al_2O_3 ratio around 10 while in phillipsite it is around 3–5.

In many of the earlier investigations, the effect of water content in the mixture has not been studied. The concentration of the reacting components in the initial mixture if expressed inversely with the water content is of significance in the determination of the species crystallized (Breck, 1974). For example, the H_2O/Na_2O ratio in the starting mixture represents the inverse of the alkalinity. The effect of this ratio on the stability of formation of mordenite is presented in rectangular coordinates in Figure 4 for the reaction temperatures of 135, 150, and 165 °C. It has been observed that the temperature, reaction time, and SiO_2/Al_2O_3 being constant, the trends of stability were in the direction: analcime to mordenite to amorphous phases with an increase in the H_2O/Na_2O ratio. A higher H_2O/Na_2O ratio in the initial mixture corresponds to lower concentrations of the various components (aluminate and silicate) in the liquid phase of the gel. This, in turn, results in the formation of a less stable phase. Conversely, lower ratios of H_2O/Na_2O in the starting mixture correspond to higher concentrations of the various components in the liquid phase, resulting in the formation of a more stable zeolite phase.

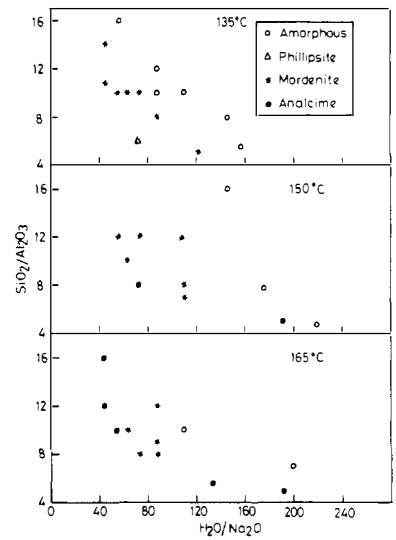

Figure 4. Batch compositions for synthesis of zeolite for 24 h in the Na_2O–Al_2O_3–SiO_2–H_2O system (rectangular coordinates).

Effect of Temperature. Although experiments were conducted at several temperature levels, only three temperatures (135, 150, and 165 °C) are used for discussion on the various aspects of the synthesis of mordenite, since it was observed that no mordenite was formed at temperatures less than 135 °C. Beyond 175 °C analcime appeared.

In Figures 1 and 2 parts a, b, and c the stability field for mordenite formation is indicated. The trends of changes with increase in temperature are indicated in the composite diagrams (Figures 1d and 2d) by superimposition of these three diagrams. It can be observed that at higher temperatures mordenite starts crystallizing from starting mixtures containing more silica or less Na_2O. This shift in crystallization field for mordenite with an increase in temperature of synthesis can be explained as follows. The concentrations of components (aluminate and silicate) in the liquid phase of the gel is the main controlling factor in the formation of a zeolite (Zhdanov, 1971). As the temperature increases, the solubilities of the aluminate and silicate ions increase, causing a shift in the concentration of the liquid phase. This results in the formation of analcime in place of mordenite. Hence if the mordenite has to be crystallized at higher temperature, the starting mixtures should have relatively higher SiO_2 or lower Na_2O contents, which means the reduction of the alkalinity.

The sequence of formation of the products with an increase in temperature is in the direction: amorphous to mordenite to analcime. For instance, for the runs at

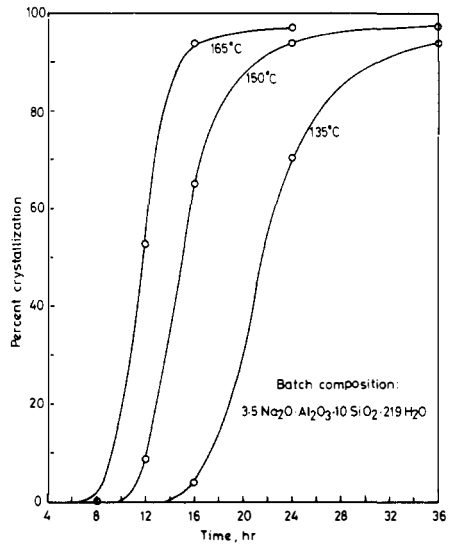

Figure 5. Crystallization curves of mordenite.

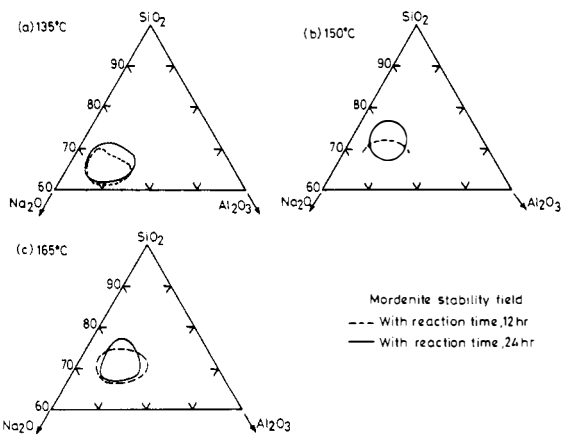

Figure 6. Effect of time on the stability field of mordenite.

temperatures of 135, 150, and 165 °C for a reaction period of 24 h the products obtained were mordenite at 135 °C and analcime at 150 and 165 °C, the initial composition being the same ($3Na_2O{\cdot}Al_2O_3{\cdot}8SiO_2{\cdot}219H_2O$).

The rate curve established on the basis of quantitative analysis of the X-ray diffraction data are shown in Figure 5. For any mixture, as the temperature increases, the rate of crystallization of mordenite increases.

Effect of Duration of Reactions. For the temperatures 135, 150, and 165 °C, the mordenite crystallization field for 12 and 24 h of reaction time are indicated in Figure 6. As the reaction time increased, the sequence of formation of product was in the direction: amorphous to phillipsite/mordenite to analcime. Such an observation is in conformity with the earlier works (Barrer, 1948, 1952; Coombs et al., 1959). In the above, analcime was the most stable phase. This trend indicates that less stable species nucleate more rapidly than the more stable ones. According to the Ostwald's law of successive transformation, the most stable state may not be reached at once, but passes through a succession of intermediate and less stable states. This correlates with the idea that the phases tend to appear in the order of decreasing simplexity or entropy (Goldsmith, 1953). Ready nucleation may be favored by high simplexity or entropy. However, the energy as well as the entropy changes ultimately determine the relative stabilities of the phases formed and hence the final product.

Crystallization Mechanism and Kinetics. The crystallization curves for mordenite at different temperatures with a fixed batch composition of $3.5Na_2O{\cdot}Al_2O_3{\cdot}10SiO_2{\cdot}219H_2O$ are indicated in Figure 5. These curves are characterized by a sigmoidal shape indicative of long induction periods followed by a rapid crystallization ultimately reaching an asymptotic value. Once the crystallization has started, the fast conversion rate of the amorphous batch into mordenite indicates that the rate-limiting step in the overall process is the nucleation. The crystallization curves compare well in their nature to the one reported by Culfaz and Sand (1973) for the formation of mordenite.

Table I. Activation Energies for Nucleation and Crystal Growth of Mordenite

source	temp range, °C	activation energy, kcal/g-mol: nucleation	activation energy, kcal/g-mol: crystal growth
present study	135-165	10.2	7.6
Domine and Quebex (1968)	250-290	11.0	
Culfaz and Sand (1973)	90-135	24.0	15.0

The activation energy for the nucleation and crystal growth are determined from the crystallization curves. Assuming that the formation of nuclei of a stable size (which do not redissolve but grow into a crystal) is an energetically activated process and since the nucleation during the induction period is the rate-determining process, the apparent activation energy for the nucleation, E_n, can be calculated from the expression

$$\frac{d \ln (1/\theta)}{d(1/T)} = -\frac{E_n}{R}$$

where θ is the induction time, i.e., the point on the crystallization curve where conversion to the crystalline phase is just starting (Hsu, 1971), T is the temperature, and R is the gas constant.

A similar analysis is made for the crystallization rate in determining the apparent activation energy, E_c, for the crystal growth assuming that the rate-limiting step is the crystal growth. This is most nearly true when the conversion rate is the highest; therefore, the crystallization rate is defined as the rate of conversion at 50% of the total conversion level in terms of percent crystallization per hour. The results obtained from these analyses are compared with the literature value in Table I.

The activation energy values obtained for nucleation in the present investigation are in the range indicated by Domine and Quobex (1968). However, the values of 24 kcal/g-mol (for nucleation) and 15 kcal/g-mol (for crystal growth) reported by Culfaz and Sand (1971) are too high compared to the values in the present work. The X-ray powder data, cell constants, IR absorption spectra, DTA and TGA, and other characterization results are presented elsewhere (Bajpai, 1977).

Acknowledgment

Valuable discussions with Professor E. C. Subba Rao, Materials Science Department, IIT-Kanpur, are gratefully acknowledged. The financial assistance provided by the Council of Scientific and Industrial Research (India) to P.K.B. in the form of a fellowship is gratefully acknowledged.

Literature Cited

Allan, D., Voorhies, A., Jr., *Ind. Eng. Chem. Prod. Res. Dev.*, **11**, 159 (1972).
Ames, L. L., Jr., Sand, J. B., *Am. Mineral*, **43**, 4776 (1958).
Bajpai, P. K., Ph.D. Thesis, Indian Institute of Technology, Kanpur, 1977.
Barrer, R. M., *J. Chem. Soc.*, 127 (1948).

Barrer, R. M., White, E. A. D., *J. Chem. Soc.*, 1261 (1951).
Barrer, R. M., White, E. A. D., *J. Chem. Soc.*, 1561 (1952).
Barrer, R. M., *Chem. Ind.*, **7**, 1203 (1968).
Breck, D. W., "Zeolite Molecular Sieves", Wiley, New York, N.Y., 1974.
Brecker, K. A., Karge, H. G., Streubel, W. D., *J. Catal.*, **28** (3), 403 (1973).
Brooks, C. S., *Adv. Chem. Ser.*, **No. 102**, 426 (1971).
Coombs, D. S., Ellis, A. J., Fyfe, W. F., Taylor, A. M., *Geochim. Cosmochim. Acta.*, **17**, 53 (1959).
Culfaz, A., Sand, L. B., *Adv. Chem. Ser.*, **No. 121**, 140 (1973).
Domine, D., Quobex, J., "Molecular Sieves", p 10, Society of Chemical Industry, London, 1968.
Freund, E. F., *J. Cryst. Growth*, **34**, 11 (1976).
Goldsmith, J. R., *J. Geol.*, **61**, 439 (1953).
Hansford, R. C., Ward, J. W., *J. Catal.*, **13**, 316 (1969).
Hopper, J. R., Shigemura, D. S., *AIChE J.*, **19**, 1025 (1973).
Hsu, A. C. T., *AIChE J.*, **17**, 1311 (1971).
Karge, H. G., "Symposium on the Mechanism of Hydrocarbon Reactions", p 417, Siofox, Hungary, June 5–7, 1973.
Kawasaki, A., Taniguchi, M., Nishiyawa, T., Japanese Patent 7 109 593 (Mar 11, 1971); *Chem. Abstr.*, **75**, 37612C (1971).
Keough, A. N., Sand, L. B., *J. Am. Chem. Soc.*, **83**, 3536 (1961).
Kladning, W. F., *Acta Cient Venez.*, **26**, 40 (1975).
McLachlan, D., Jr., "X-ray Crystal Structure", p 10, McGraw-Hill, New York, N.Y., 1957.
Meier, W. M., *Z. Krist.*, **115**, 439 (1961).
Meier, W. M., "Molecular Sieves", p 10, Society of Chemical Industry, London, 1968.
Miale, J. N., Weisz, P. B., *J. Catal.*, **20**, 288 (1971).
Norton Co., Neth. Appl. 298 606 (Cl. Colb) (Aug 10, 1965); *Chem. Abstr.*, **64**, 4656a (1966).
Rao, C. N. R., "Chemical Applications of Infra-red Spectroscopy", Academic Press, New York, N.Y., 1963.
Sand, M. L., Coblenz, W. S., Sand, L. B., *Adv. Chem. Ser.*, **No. 101**, 127 (1971).
Tatsuaki, Y., Hura, M., Nobuyoshi, H., *Bull. Jpn. Pet. Inst.*, **12** (1970).
Voorhies, A., Jr., Hopper, J. R., *Adv. Chem. Ser.*, **No. 102**, 410 (1971).
Wolf, F., Renning, J., East German Patent 83978 (Cl. Colb) (Aug 20, 1971); *Chem. Abstr.*, **78**, 113434y (1973).
Zhdanov, S. P., *Adv. Chem. Ser.*, **No. 101**, 20 (1971).

Received for review December 29, 1977
Accepted May 18, 1978

Hydrogenation of Dicyanobutene to Adiponitrile with Palladium-on-Charcoal

Richard T. Stimek and Howard F. Rase*

Department of Chemical Engineering, The University of Texas at Austin, Austin, Texas 78712

The deactivation characteristics of palladium-on-charcoal in the hydrogenation of dicyanobutene (DNB) to adiponitrile have been studied at conditions of industrial interest where all three modes of deactivation occurred simultaneously. The catalyst is reversibly poisoned by H_2S generated from the charcoal itself, deactivated by a nitrogenous coke formed from the DNB, and deactivated by sintering. The coke deposit and the H_2S accelerated sintering. A means for reactivating the catalyst using water addition was developed. Currently accepted hypotheses and theories on deactivation along with X-ray, ESCA, and electron microscopy aided in analyzing the complex and interacting deactivation patterns.

It is now generally agreed that catalyst deactivation occurs by sintering, fouling, or poisoning. Many excellent studies have been reported using simple reactions and carefully controlled environments in order to isolate and define a specific mode of deactivation. The insights provided by these efforts, which have been competently reviewed (Butt, 1972), are valuable in analyzing the more complex situation in an industrial reaction, where all three modes of deactivation often occur simultaneously and, at times, interactively. Although references to general deactivation patterns of certain industrial reactions appear, few definitive studies have been presented. However, it is reasonable to assume that, just as in the study of reaction kinetics, observations on complex real systems can lead to new and valuable insights.

The research to be described was undertaken not only to define the deactivation characteristics for an industrially important system but also to demonstrate the utility of existing techniques and concepts in discovering causes for deactivation and in developing practical procedures for maximizing catalyst life. The system studied employed a 0.2% Pd-on-charcoal catalyst in the catalytic hydrogenation of dicyanobutene (DNB) to adiponitrile (ADN), an important intermediate in the production of nylon.

General Process Description

As described by Bailey (1971), Hillyear and Stallings (1956), and Sherwood (1963), 1,4-dicyano-2-butene, which is obtained via the chlorination of butadiene to dichlorobutenes followed by cyanation, is hydrogenated in the vapor phase to adiponitrile over 0.2% Pd-on-charcoal catalyst using inlet temperatures in the range of 250–300 °C. The product is obtained by cooling and condensation, and the hydrogen is recycled. High conversion and selectivity are necessary because separation of unreacted DNB is not feasible.

One would expect that all three methods of deactivation might occur in this system because of the well-known tendency of unsaturated hydrocarbons to form both thermal and catalytic coke (Oblad et al., 1940), the susceptibility of platinum metals to poisoning (Maxted, 1951), and the sensitivity of palladium to sintering (Pope et al., 1971). However, the specific quantitative effects and possible interactions between modes of deactivation can only be determined by careful experimental studies on the particular system of interest. Accordingly, all three modes of deactivation were investigated. The insights gained suggested improved operating conditions for minimizing catalyst deactivation.

Experimental Equipment and Procedures

Catalyst. The catalyst used was a nominal 0.2 wt % palladium deposited on coconut-shell charcoal.

Hydrogenation Reaction System. Conversion studies were conducted utilizing a laboratory hydrogenation system. The hydrogenation reactor was built from two 12 in. long sections of 4-in. schedule 40 stainless steel pipe joined together with a $1^1/_4$-in. steel disk. This arrangement

0019-7890/78/1217-0227$01.00/0